Accurate Analysis of Polarization Coupling in Laminated Multilayered Thin Film Optical 3-D Waveguides

A. Massaro, V. Mancini, A. Di Donato and T. Rozzi

Departement of Electronics and Automatics, University of Ancona, Via Brecce Bianche, 60131, e-mail: MassaroAle@libero.it, a.didonato@ee.unian.it

***Abstract* — Coupled mode theory (CM) is widely applied in integrated optics, while the rigorous Local Mode theory (LM) is less known, being somewhat harder to implement. We compare the two theories in determining polarization coupling inside a laminated rib waveguide made of a-Si:H and SiO_2.For moderate optical axis slant (low hybridization) and for fixed layer thickness the two theories show similar results but LM becomes mandatory when hybridization is important.**

I. INTRODUCTION

In the realization of integrated optical circuits, single mode, polarization maintaining three-dimensional dielectric waveguides have great importance. The property of maintaining the polarization can be ensured by using of thin multilayer films which induce artificial birefringence [8]. The structure analysed consist of a very thin film lamination (a-Si:H, SiO_2) of layers of different refractive indeces alternating periodically high (n_2) and low (n_1) values, exhibiting birefringence, as shown in figure 1. The optical axis of the artificial anisotropic dielectric is perpendicular to the lamination and slanted an angle ϑ from the z direction. Infact we will analyze a waveguide that supports a single LSE mode and a single LSM mode, these will couple owing to the presence of the grating along the longitudinal axis created by the slant. We will consider in particular the negative uniaxial optical behaviour of laminated polarization beam-splitters (LPS) [1]-[8]. By means of the Effective Dielectric Constant (EDC) method we will determine the geometrical parameters of the rib waveguide in order to get a single LSE and a single LSM mode in propagation at the wavelength of 1.55μm, and we will represent the dielectric constant $\varepsilon(x,z)$ inside the laminated guiding core as a square wave along the direction normal to the layers.

II. METHOD OF ANALYSIS

The five-component solution for an LSE (or LSM) mode can be expressed in terms of an Hertz vector, π_h (or π_e), directed along the y –axis .$\pi_h(x,y)$ is infact, proportionals to H_y whilst $\pi_e(x,y)$ is proportional to E_y. The scalar potential $\pi_{h,e}$ satisfy the wave equation:

$$\partial_x^2 \pi_{h,e}(x,y) + \partial_y^2 \pi_{h,e}(x,y) + (\varepsilon_r \kappa_0^2 - \beta^2)\pi_{h,e}(x,y) = 0 \quad (1)$$

The five-component solution for both LSE and LSM can be found according to:

$$\begin{aligned} E_x &= \omega\mu_0\beta\pi_h + \partial_x\partial_y\pi_e & E_y &= (\varepsilon_r k_0^2 + \partial_y^2)\pi_e \\ H_x &= \partial_x\partial_y\pi_h - \omega\varepsilon\beta\pi_e & H_y &= (\varepsilon_r k_0^2 + \partial_y^2)\pi_h \\ H_z &= j\omega\varepsilon\partial_x\pi_e - j\beta\partial_y\pi_h \end{aligned} \quad (2)$$

The local modes are defined as the eigenfunctions of a locally uniform waveguide along the longitudinal axis having the same cross-section as the actual guide at the plane considered. Therefore, local modes are solutions of the transverse wave equation:

$$\partial_x^2\varphi_n + \partial_y^2\varphi_n + (\varepsilon_r\kappa_0^2 - \beta^2)\varphi_n = 0 \quad (3)$$

We use the local mode theory starting from Maxwell equation in the rectangular coordinate system of figure 1, [9],[10].

$$-\partial_z \mathbf{E_t} + \nabla_t \frac{(\hat{z}\cdot\nabla_t \times \mathbf{H_t})}{j\omega\varepsilon(x,z)} = j\omega\mu_0 \mathbf{H_t}\times\hat{z} \quad (4a)$$

$$-\partial_z \mathbf{H_t} + \frac{[\nabla_t\nabla_t\cdot(\hat{z}\times\mathbf{E_t})]}{j\omega\mu_0} = j\omega\varepsilon(x,z)\cdot(\hat{z}\times\mathbf{E_t}) \quad (4b)$$

The LSE/LSM fields, of the rib waveguide in question, are reported in table I. By neglecting the radiation modes of the rib waveguide, the global transverse field of the laminated rib at any point $z=z_0$ can be expressed as a superposition of the discrete components in the two polarizations

$$\mathbf{E_t}(x,y,z) = \sum_n V_n(z)\mathbf{E}_n(x,y) \quad (5a)$$

$$\mathbf{H_t}(x,y,z) = \sum_n I_n(z)\mathbf{H}_n(x,y) \qquad (5b)$$

The local eigenmodes $\mathbf{E}_n(x,y)$ and $\mathbf{H}_n(x,y)$ in eqn.5 are orthonormalised as follow :

$$\int_S \mathbf{E}_n \times \mathbf{H}_n \cdot \hat{z}\, ds = \begin{matrix} 1 \text{ if } m = n \\ 1 \text{ if } m \neq n \end{matrix} \qquad (6)$$

where the integration is carried out over the entire cross-section S of the guide. Starting from (4) and utilizing (6) we obtain the following coupled transmission line equation:

$$\frac{dV_m(z)}{dz} = -j\sum X_{mn} I_n(z) \qquad (7a)$$

$$\frac{dI_m(z)}{dz} = -j\sum B_{mn} V_n(z) \qquad (7b)$$

The reactance (X) and the susceptance (B) matrices per unit length are defined as

$$X_{mn} = \int_s [\omega\mu(HH_{ny}H_{my} + H_{nx}H_{my}) + \frac{1}{\omega}H_{mx}\,\partial_y \frac{\partial_y H_{nx}}{\varepsilon}]dS\,,$$

$$B_{mn} = \omega\int_s \varepsilon(E_{ny}E_{my} + E_{nx}E_{mx})\,dS + \frac{1}{\omega\mu}\int_s E_{mx}\,\partial_y^2 E_{nx}\,dS \qquad (8)$$

For LSE modes we used the ordinary refractive index n_o , whereas for LSM modes we used $n_e(\vartheta)$[1]-[8].

$$n_o = \left(\frac{d_1\varepsilon_1 + d_2\varepsilon_2}{d_1 + d_2}\right)^{1/2} \qquad (9a)$$

$$n_e(\vartheta) = \left(\frac{{n_o}^2 \cdot {n_e}^2}{{n_o}^2 \cdot \sin^2(\vartheta) + {n_e}^2 \cdot \cos^2(\vartheta)}\right)^{1/2} \qquad (9b)$$

where:

$$n_e = \left(\frac{(d_1 + d_2)\cdot\varepsilon_1\varepsilon_2}{d_1\varepsilon_2 + d_2\varepsilon_1}\right)^{1/2} \qquad (9c)$$

We observe that the subscript 1 is referred to SIO_2 and the subscript 2 is referred to a-SI:H. With respect to the '1Ω' normalised mode impedance for both modes under the present normalization scheme, the modal amplitudes can be expressed in terms of forward travelling waves with with amplitudes a_n and backward travelling waves with amplitudes b_n :

$$a_n = (V_n + I_n)/2 \qquad (10a)$$

n=1,2.

$$b_n = (V_n - I_n)/2 \qquad (10b)$$

The subscript 1 below will designate the LSE mode while the subscript 2 will be associated to the LSM mode. Under the above hypotheses ,substituting (9) in (7) yields :

$$da_1/dz = -j\beta_1 \cdot a_1 - jc \cdot a_2 \qquad (11a)$$

$$da_2/dz = -j\beta_2 \cdot a_2 - jc \cdot a_1 \qquad (11b)$$

where :

$$\begin{aligned} \beta_1 &= (X_{11} + B_{11})/2 \\ c &= (X_{12} + B_{12})/2 \\ \beta_2 &= (X_{22} + B_{22})/2 \end{aligned} \qquad (12)$$

c is the coupling coefficient between modes of different polarizations. In order to evaluate the coupling coefficient we represent ε(x,z) as a square wave along the direction normal to the layers :

$$\varepsilon(x,z) = \frac{(\varepsilon_1 d_1 + \varepsilon_2 d_2)}{d_1 + d_2} + \sum_{n=1}^{\infty} E_n + F_n \qquad (13)$$

where:

$$E_n = \frac{(\varepsilon_2 - \varepsilon_1)}{n\pi}\sin\left(\frac{2n\pi\pi_2}{\Lambda}\right)\cos\left(\frac{n\pi\pi(x\cdot\sin(\vartheta) + z\cdot\cos(\vartheta))}{\Lambda}\right),$$

$$F_n = \frac{(\varepsilon_2 - \varepsilon_1)}{n\pi}\cos\left(\frac{2n\pi\pi_2}{\Lambda}\right)\sin\left(\frac{n\pi\pi(x\cdot\sin(\vartheta) + z\cdot\cos(\vartheta))}{\Lambda}\right) \qquad (14)$$

$\Lambda = d_1 + d_2$ and ϑ is the optical axis, as shown in figure 1.b. The Fourier coefficients can be found as:

$$a'_0 = \frac{2}{\Lambda}\cdot\int_0^{\Lambda} f(x)\,dx = \frac{2}{\Lambda}\cdot(\varepsilon_1 d_1 + \varepsilon_2 d_2) \qquad (15a)$$

$$a'_n = \frac{2}{\Lambda}\cdot\int_0^{\Lambda} f(x)\cdot\cos(\frac{2n\pi\pi}{\Lambda})\,dx = \frac{\varepsilon_2 - \varepsilon_1}{n\pi}\cdot\sin(\frac{2n\pi\pi_2}{\Lambda}) \qquad (15b)$$

$$b'_n = \frac{2}{\Lambda}\cdot\int_0^{\Lambda} f(x)\cdot\sin(\frac{2n\pi\pi}{\Lambda})dx = \frac{\varepsilon_2 - \varepsilon_1}{n\pi}\cdot\left(1 - \cos(\frac{2n\pi\pi_2}{\Lambda})\right) \qquad (15c)$$

where f(x) represents the index distribution along the direction normal to the layers:

$$f(x) = \frac{a_0'}{2} + \sum_{n=1}^{\infty}\left[a_n' \cdot \cos\frac{2n\pi\pi}{\Lambda} + b_n' \cdot \sin\frac{2n\pi\pi}{\Lambda} \right] \qquad (16)$$

III. RESULTS

For the rib waveguide the dimensions, as in figure 1.a and 1.b, are : w =1.2 μm , t =0.4 μm , D =1 μm , d =0.6 μm , θ =20°, d_1=100nm, d_2=8nm, $n_1(SiO_2)$=1.465, n_2(a-Si:H)=3.24, n_s(substrate)=3. These values guarantee the presence of just one LSE and one LSM mode propagating in the dielectric waveguide.

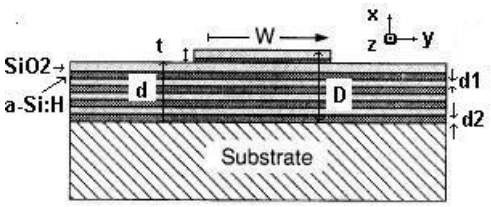

Fig.1a: Cross-section of the laminated rib.

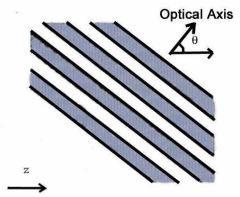

Fig. 1b: Optical axis perpendicular to the laminated layers and slanted at an angle ϑ from the z direction

It is evident in figure 4b that, varying z from 0 to 90 nm, the values of curves become more similar. Figure 2 shows the coupling coefficient C(z) between the LSE and LSM mode for the two theories, [11],[12]. The positions of maxima and minima nearly coincide. The difference between amplitudes can be explained considering that the LM theory takes into account field hybridization losses, owing to the undesired coupling between the hybrid field components due to the discontinuity caused by the lamination.

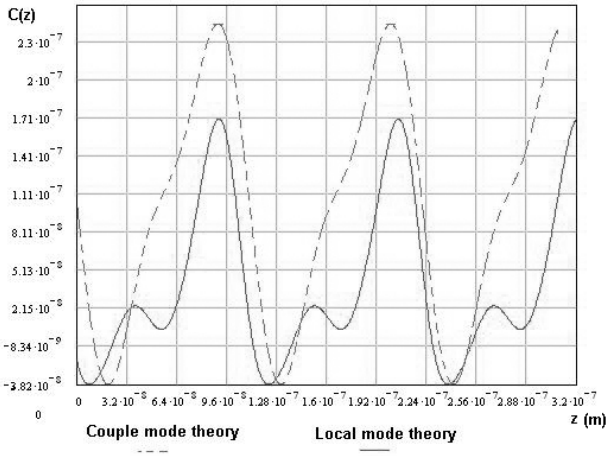

Fig.3: Coupling coefficient (θ=20°)

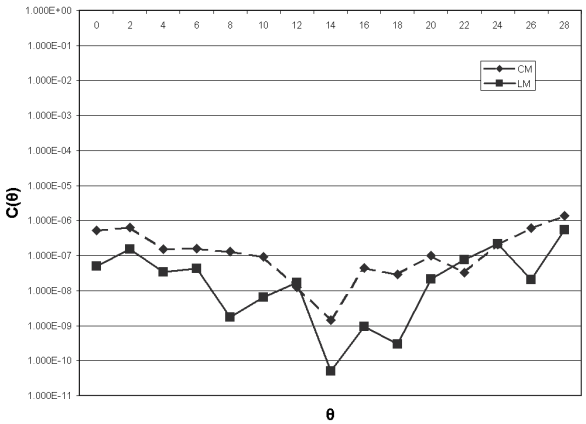

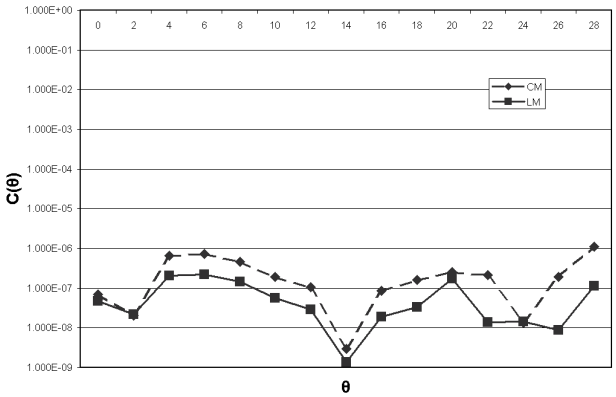

Fig.4b Coupling coefficient varying with θ at z=90.56nm

In figure 4.a and in figure 4.b are reported the curves of C(θ) computed at z = 0 and z = 90.56 nm respectively.

TABLE I
LSE – LSM Potentials in the guiding region

	LSE	LSM
$\mathbf{E_x}$	$\omega\mu_0\beta_{lse}\cdot\frac{\cos(K_{xlse}\cdot x-\varphi_{xlse})}{\cos(K_{xlse}\cdot w-\varphi_{xlse})}\cdot\frac{\cos(K_{yIIIse}\cdot y-\varphi_{IIIse})}{\cos(K_{yIIIse}\cdot D-\varphi_{IIIse})}$	$K_{xlsm}K_{yIIIsm}\cdot\frac{\sin(K_{xlsm}\cdot x-\varphi_{xlsm})}{\cos(K_{xlsm}\cdot w-\varphi_{xlsm})}\cdot\frac{\cos(K_{yIIIsm}\cdot y-\varphi_{IIIsm})}{\cos(K_{yIIIsm}\cdot D-\varphi_{IIIsm})}$
$\mathbf{E_y}$		$\left(\varepsilon_r K_0^2-K_{yIIIsm}{}^2\right)\cdot\frac{\cos(K_{yIIIsm}\cdot y-\varphi_{IIIsm})}{\cos(K_{yIIIsm}\cdot D-\varphi_{IIIsm})}\cdot\frac{\cos(K_{xlsm}\cdot x-\varphi_{xlsm})}{\cos(K_{xlsm}\cdot w-\varphi_{xlsm})}$
$\mathbf{E_z}$	$-j\omega\mu_0 K_{xlse}\cdot\frac{\sin(K_{xlse}\cdot x-\varphi_{xlse})}{\cos(K_{xlse}\cdot w-\varphi_{xlse})}\cdot\frac{\cos(K_{yIIIse}\cdot y-\varphi_{IIIse})}{\cos(K_{yIIIse}\cdot D-\varphi_{lse})}$	$j\beta_{lsm}K_{yIIIsm}\cdot\frac{\sin(K_{yIIIsm}\cdot y-\varphi_{IIIsm})}{\cos(K_{yIIIsm}\cdot D-\varphi_{IIIsm})}\cdot\frac{\cos(K_{xlsm}\cdot x-\varphi_{xlsm})}{\cos(K_{yIIIsm}\cdot w-\varphi_{lsm})}$
$\mathbf{H_x}$	$K_{xlse}K_{yIIIse}\cdot\frac{\sin(K_{xlse}\cdot x-\varphi_{xlse})}{\cos(K_{xlse}\cdot w-\varphi_{xlse})}\cdot\frac{\sin(K_{yIIIse}\cdot y-\varphi_{IIIse})}{\cos(K_{yIIIse}\cdot D-\varphi_{lse})}$	$-\omega\varepsilon\beta_{lsm}\cdot\frac{\cos(K_{xlsm}\cdot x-\varphi_{xlsm})}{\cos(K_{xlsm}\cdot w-\varphi_{xlsm})}\cdot\frac{\cos(K_{yIIIsm}\cdot y-\varphi_{IIIsm})}{\cos(K_{yIIIsm}\cdot D-\varphi_{IIIsm})}$
$\mathbf{H_y}$	$\left(\varepsilon_r K_0^2-K_{yIIIse}{}^2\right)\cdot\frac{\cos(K_{yIIIse}\cdot y-\varphi_{IIIse})}{\cos(K_{yIIIse}\cdot D-\varphi_{IIIse})}\cdot\frac{\cos(K_{xlse}\cdot x-\varphi_{xlse})}{\cos(K_{xlse}\cdot w-\varphi_{xlse})}$	
$\mathbf{H_z}$	$j\beta_{lse}K_{yIIIse}\cdot\frac{\sin(K_{yIIIse}\cdot y-\varphi_{IIIse})}{\cos(K_{yIIIse}\cdot D-\varphi_{IIIse})}\cdot\frac{\cos(K_{xlse}\cdot x-\varphi_{xlse})}{\cos(K_{yIIIse}\cdot w-\varphi_{lse})}$	$-j\omega\varepsilon K_{xlsm}\cdot\frac{\sin(K_{xlsm}\cdot x-\varphi_{xlsm})}{\cos(K_{xlsm}\cdot w-\varphi_{xlsm})}\cdot\frac{\cos(K_{yIIIsm}\cdot y-\varphi_{IIIsm})}{\cos(K_{yIIIsm}\cdot D-\varphi_{lsm})}$

As shown in figure 3 the positions of the peaks moves as z varies, and for fixed values of z they may coincide, but in all figures is evident as the LM theory has an amplitude smaller respect to the CM theory (power losses).

V. CONCLUSION

In summary, we have compared two different theories in order to analyze thin multilayer films rib waveguide, as utilized in all optical systems where polarization control is required (e.g. integrated passive optical polarization switches and isolators). This study shows clearly that in order to model accurately this integrated structure we have to use the rigorous LM theory, as it considers the coupling of the hybrid field components owing to the slanted thin films lamination.

REFERENCES

[1] B.Rossi, Optics, Addison-Wesley, Reading, Chap.6, 1967.

[2] K. Shiraishi, K. Matsumura "Fabrication of spatial walk-off polarizing film by oblique depositions", Journal of Quantum Electronics, Vol. 30 pp. 2417-2420, October 1994.

[3] K. Shiraishi, S. Kawakami, "Spatial walk-off polarizer utilizing artificial anisotropic dielectrics", Optics Letters, Vol. 15 pp. 516-518, May 1990.

[4] T. Sato, T.Sasaki, K. Tsutchida, K. Shiraishi, S. Kawakami, "Scattering mechanism and reduction of insertion losses in a laminated polarization splitter", Applied Optics, Vol. 33 pp. 6925-6934, October 1994.

[5] K. Shiraishi, K. Mura "Poly Si/SiO2 laminated Walk-Off Polarizer Having a Beam-Splitting Angle of More Than 20° ", Journal Of Lightwave Technology, Vol. 16 pp. 127-133, January 1998.

[6] M. Born, E. Wolf ,Principles of Optics, U.K. Pergamon, Chap. XIV, 1980.

[7] K. Shiraishi, T. Sato, S. Kawakami, K. Tsutchida, "Laminated polarization splitter with a large split angle" , Appl. Phys. Lett., Vol. 61 pp. 2633-2634, November 1992.

[8] A. Massaro, A. Di Donato, T.Rozzi, "Negative uniaxial optical behaviour of laminated polarization beam-splitters" GaAs2002 Conference, Milan, pg.133.

[9] T. Rozzi, M. Mongiardo "Open E.M. Waveguides" IEE, Press London 1999.

[10] T.Rozzi, M. Farina, "Advanced Electromagnetic Analysis of passive and active planar structures", IEE, Cap2, pp.26-29.

[11] Shevchenko, V.V. "Continuous trasitions in open waveguides", Golem Press, 1971.

[12] Marcuse "Theory of dielectric optical waveguides", Academic Press, 1974.